

Accepted Manuscript

Fragmentation of GW4064 led to a highly potent partial Farnesoid X Receptor agonist with improved drug-like properties

Daniel Flesch, Matthias Gabler, Andreas Lill, Roberto Carrasco Gomez, Ramona Steri, Gisbert Schneider, Holger Stark, Manfred Schubert-Zsilavecz, Daniel Merk

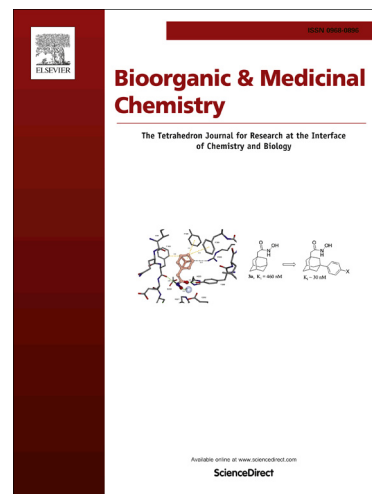
PII: S0968-0896(15)00333-8
DOI: <http://dx.doi.org/10.1016/j.bmc.2015.04.035>
Reference: BMC 12247

To appear in: *Bioorganic & Medicinal Chemistry*

Received Date: 24 January 2015
Revised Date: 24 March 2015
Accepted Date: 10 April 2015

Please cite this article as: Flesch, D., Gabler, M., Lill, A., Gomez, R.C., Steri, R., Schneider, G., Stark, H., Schubert-Zsilavecz, M., Merk, D., Fragmentation of GW4064 led to a highly potent partial Farnesoid X Receptor agonist with improved drug-like properties, *Bioorganic & Medicinal Chemistry* (2015), doi: <http://dx.doi.org/10.1016/j.bmc.2015.04.035>

This is a PDF file of an unedited manuscript that has been accepted for publication. As a service to our customers we are providing this early version of the manuscript. The manuscript will undergo copyediting, typesetting, and review of the resulting proof before it is published in its final form. Please note that during the production process errors may be discovered which could affect the content, and all legal disclaimers that apply to the journal pertain.



Graphical Abstract

Fragmentation of GW4064 led to a highly potent partial Farnesoid X Receptor agonist with improved drug-like properties

Leave this area blank for abstract info.

Daniel Flesch^{a1}, Matthias Gabler^{a1}, Andreas Lill^{a1}, Roberto Carrasco Gomez^a, Ramona Steri^a, Gisbert Schneider^b, Holger Stark^c, Manfred Schubert-Zsilavecz^a, Daniel Merk^{a*}

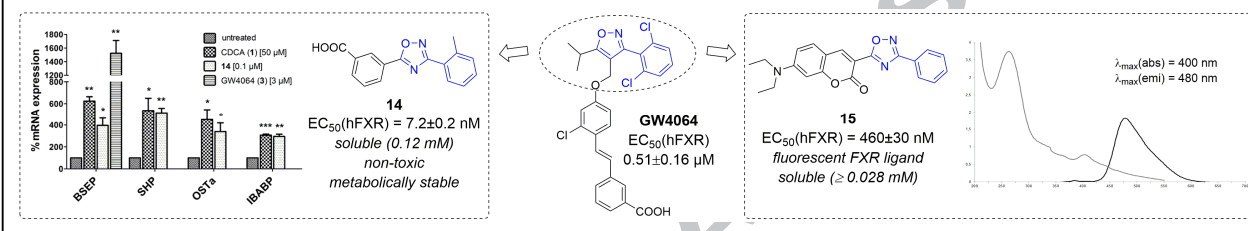
^a Institute of Pharmaceutical Chemistry, Goethe University Frankfurt, Max-von-Laue-Str.9, 60438 Frankfurt, Germany

^b Department of Chemistry and Applied Biosciences, ETH Zürich, Vladimir-Prelog Weg 1-5/10, 8093 Zürich, Switzerland

^c Institute for Pharmaceutical und Medicinal Chemistry, Heinrich-Heine-University Düsseldorf, Universitätsstr. 1, 40225 Düsseldorf, Germany

¹ DF, MG and AL contributed equally to this work and are listed in alphabetical order

*merk@pharmchem.uni-frankfurt.de, Tel.: +496979829806, Fax: +496979829332





Fragmentation of GW4064 led to a highly potent partial Farnesoid X Receptor agonist with improved drug-like properties

Daniel Flesch^{a1}, Matthias Gabler^{a1}, Andreas Lill^{a1}, Roberto Carrasco Gomez^a, Ramona Steri^a, Gisbert Schneider^b, Holger Stark^c, Manfred Schubert-Zsilavecz^a, Daniel Merk^{a*}

^aInstitute of Pharmaceutical Chemistry, Goethe University Frankfurt, Max-von-Laue-Str.9, 60438 Frankfurt, Germany

^bDepartment of Chemistry and Applied Biosciences, ETH Zürich, Vladimir-Prelog Weg 1-5/10, 8093 Zürich, Switzerland

^cInstitute for Pharmaceutical und Medicinal Chemistry, Heinrich-Heine-University Düsseldorf, Universitätsstr. 1, 40225 Düsseldorf, Germany

¹DF, MG and AL contributed equally to this work and are listed in alphabetical order *merk@pharmchem.uni-frankfurt.de, Tel.: +496979829806, Fax: +496979829332

ARTICLE INFO

ABSTRACT

Article history:

Received

Received in revised form

Accepted

Available online

Keywords:

metabolic disorders

nuclear receptors

farnesoid X receptor

FXR agonists

fluorescent FXR ligand

The ligand activated transcription factor farnesoid X receptor (FXR) is a crucial regulator of several metabolic and inflammatory pathways and its activation by agonistic ligands seems a valuable therapeutic approach for many disorders. Most known non-steroidal FXR agonists however, have limitations that hinder their clinical development and novel FXR ligands are required. Evaluation of the co-crystal structures of the widely used FXR agonist GW4064 and related compounds in complex with the FXR ligand binding domain indicated that their disubstituted isoxazole moiety is especially relevant for FXR activation. By investigation of GW4064-fragments missing the aromatic tail, we discovered a highly potent and soluble FXR agonist (**14**, ST-1892) as well as a fluorescent FXR ligand (**15**) as potential pharmacological tool.

2009 Elsevier Ltd. All rights reserved.

1. Introduction

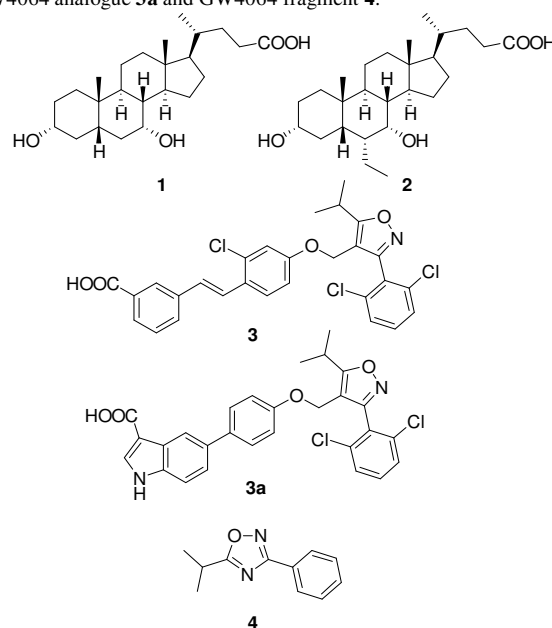
Nuclear farnesoid X receptor (FXR)¹⁻⁴ is a physiological regulator of several metabolic⁵⁻⁷ and inflammatory^{7,8} pathways. In its main role, FXR acts as a sensor for endogenous bile acids such as chenodeoxycholic acid (**1**, CDCA) and modulates bile acid synthesis, transport and metabolism.^{9,10} In addition, FXR is involved in glucose homeostasis, fatty acid transport and metabolism, liver protection, intestinal inflammation and several forms of cancer.^{5,7,9-15}

The first-in-class semisynthetic FXR agonist 6 α -ethyl-CDCA (**2**, 6-ECDCA, INT-747, OCA) has reached late stages of clinical development showing encouraging data for the treatment of the liver disorders primary biliary cirrhosis (PBC), non-alcoholic fatty liver disease (NAFLD) and non-alcoholic steatohepatitis.^{12,15-17} The clinical progress of **2** provides evidence for the value of FXR as a drug target, and besides **2** many other synthetic FXR ligands have been developed of which the GW4064 (**3**) class is most prominent (Figure 1). However, owing to the high lipophilicity of the FXR ligand binding site, most of the known FXR ligands suffer from poor aqueous solubility and bioavailability.¹⁸⁻²²

With the aim to develop new FXR agonists, we investigated the possibility of fragmenting the well-known FXR agonist GW4064 (**3**) as a basis for molecular design. After several optimization steps, we discovered a potent low-molecular weight FXR agonist that showed good solubility and low cellular

toxicity. In addition, we report a fluorescent FXR ligand as an *in vitro* pharmacological tool.

Figure 1: FXR agonists CDCA (**1**), 6-ECDCA (**2**), GW4064 (**3**), GW4064 analogue **3a** and GW4064 fragment **4**.



2. Results & Discussion

The investigation of co-crystal structures (3FXV, 3HC6, 3HC5, 3RVF, 3RUU, 3RUT, 3P88, 3P89, 3DCT, 3DCU, 3GD2)²¹⁻²⁵ of GW4064 (**3**) and analogues (**3a**) in complex with the FXR ligand-binding domain (FXR-LBD) revealed that the 5-isopropyl-3-phenylisoxazole moiety incorporated in all derivatives of **3** is bound near helices 11 and 12. The various large aromatic substituents at the 4-position of the isoxazole core are placed between helices 3, 6 and 7. For nuclear receptor activation the activation function 2 (AF-2) in helix 12 is especially important. We consequently assumed that the 3,5-disubstituted isoxazole moiety of the GW4064 scaffold might be sufficient for FXR activation.

In an initial computational docking study GW4064-fragment **4** was placed into the same region as the disubstituted isoxazole moiety of **3** (Figure 2). We therefore developed a series of GW4064 analogues lacking the aromatic 4-substituent and determined FXR modulation (**4-15**, Table 1). Moreover, the crystal structures indicated that the 2,6-dichlorophenyl substituent in 3-position of the isoxazole moiety entirely fills the available pocket near helix 6, while more space seemed available towards helix 12 around the isopropyl residue in 5-position of the isoxazole (Figure 2). Therefore, we focused on replacing the isopropyl substituent with larger aromatic moieties.

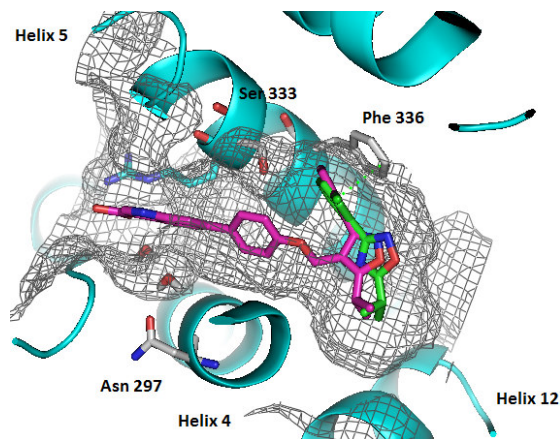


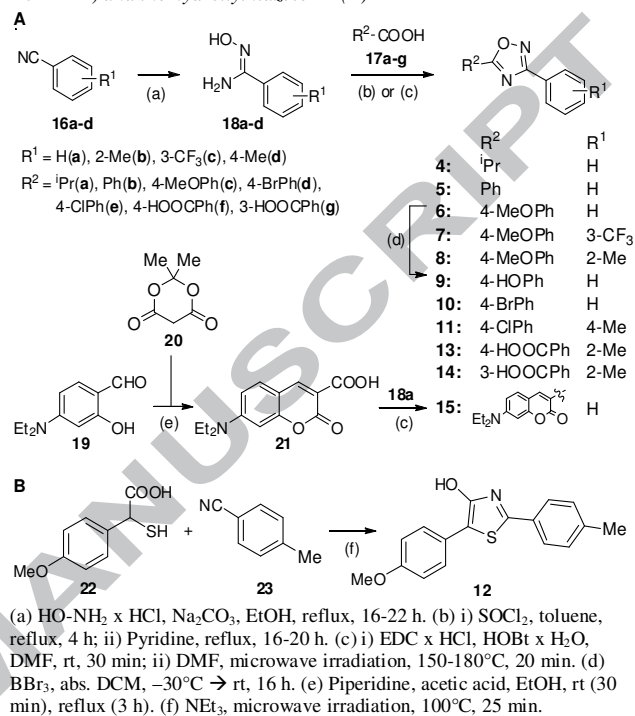
Figure 2: Crystal structure of **3a** (pink) in complex with the FXR-LBD (PDB-ID: 3RUU²¹). The isoxazole moiety of **3a** and its two substituents are directed towards helices 11 and 12 which are essential for FXR activation. Docking of oxadiazole **4** (green) suggested a binding mode very similar to the position of the disubstituted isoxazole of **3a**. Moreover, the docking pose of **4** indicated that more space (mesh represents solvent-accessible surface) is available towards helix 12 than the isopropyl substituent occupies.

2.1. Synthesis

Since we required derivatives of **3** without a substituent at position 4 of the isoxazole core, we selected a 1,2,4-oxadiazole moiety as central aromatic ring instead. Compared to the isoxazole, the oxadiazole ring offers an easier preparation and greater polarity but has a comparable size and geometry as the isoxazole. 1,2,4-Oxadiazoles (**4-11**, **13-15**) were prepared in a convergent synthesis from nitriles (**16a-d**) and carboxylic acids (**17a-g**) as starting materials.²⁶ After activation with thionyl chloride or EDC/HOBt the carboxylic acids (**17a-g**) were reacted with amidoximes (**18a-d**) to form the oxadiazole ring under microwave irradiation. The required amidoximes (**18a-d**) were generated from the respective nitriles (**16a-d**) and hydroxylamine hydrochloride. Treatment of the aromatic ether **6** with boron tribromide yielded the phenol **9**. The synthesis of fluorescent

derivative **15** started with the Knoevenagel condensation²⁷ of aldehyde **19** with Meldrum's acid (**20**) yielding coumarin derivative **21** which was suitable for reaction with amidoxime **18a** to form **15** (Scheme 1). The hydroxythiazole **12** was prepared by microwave-assisted condensation of thioglycolic acid **22** and toluonitrile (**23**).

Scheme 1: Synthesis of 1,2,4-oxadiazoles **4-11** and **13-15** (**A**) (derived from ²⁶⁻²⁸) and the hydroxythiazole **12** (**B**)



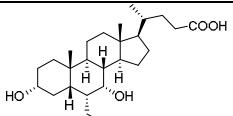
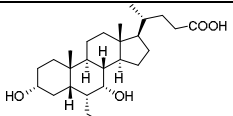
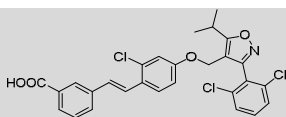
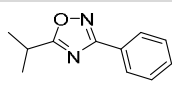
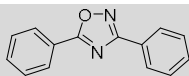
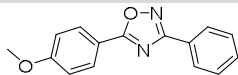
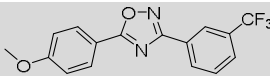
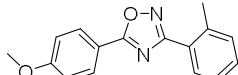
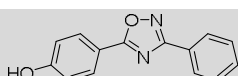
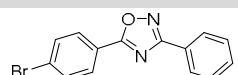
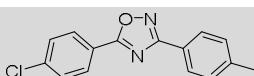
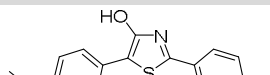
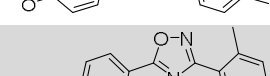
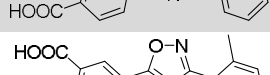
2.2. Biological evaluation & structure-activity relationship

We determined FXR activity of **4-15** (table 1) in a full length FXR reporter gene assay in HeLa cells that were transiently transfected with hFXR (constitutively expressed, CMV promoter), hRXR (constitutively expressed, SV40 promoter), a firefly luciferase (reporter gene) under the control of a shortened construct of the FXR target gene BSEP promoter and a constitutively expressed renilla luciferase with SV40 promoter as internal control of transfection efficiency, cell viability and toxicity. Compound **3** (3 μM) served as positive control (100% FXR activation, EC₅₀ of **3** in our test system: 0.51±0.16 μM). The assay was validated with **1** (EC₅₀ = 18±1 μM, 88±3% maximum relative FXR activation) and **2** (EC₅₀ = 0.16±0.02 μM, 87±3% max.).²⁹

The smallest GW4064-fragment **4** with 3-phenyl and 5-isopropyl substituents at the oxadiazole core already exhibited slight FXR activating activity and strengthened our hypothesis that especially the disubstituted isoxazole moiety accounts for the observed FXR agonism of GW4064 (**3**). To improve its potency and evaluate the SAR, we selectively varied the two substituents at the oxadiazole core structure. By introduction of two phenyl residues in **5** the FXR affinity was improved to an EC₅₀ value of 0.53±0.11 μM which suggested that additional space was available at this position inside the FXR ligand binding pocket. Interestingly, an additional methoxy group in position 4 of the 5-phenyl substituent (**6**) led to antagonistic potency in competition with **3** indicating that **6** still binds to the FXR-LBD but fails to stabilize the LBD sufficiently for activation of the nuclear receptor.

When an additional substituent was introduced at the second (3-)aromatic ring in 3- (**7**) or 2-position (**8**) the compounds exhibited partial agonistic activity again and in case of **8** the affinity was strongly improved with an EC₅₀ value of 0.12±0.01 μM. The higher affinity of **8** might be best explained by steric interactions of the methyl group in *ortho*-position with the oxadiazole moiety which causes the phenyl substituent flip out of the plane of the central aromatic ring. In **3** and derivatives a similar geometry is achieved by the 2,6-dichloro substitution.

Table 1: *In vitro* FXR-activity of **4-15** compared with **2** and **3** (mean±SEM, n=3-6). Inactive compounds showed neither agonistic nor antagonistic activity.

Compound ID		EC ₅₀ [μM] (max. rel. activation [%])
2		0.16±0.02 (87±3)
3		0.51±0.16
4		12.3±0.6% @ 50 μM [p<.001]
5		0.53±0.11 (18.6±0.8)
6		IC ₅₀ = 16.4±2.6 μM
7		2.9±0.4 (11.4±0.5)
8		0.12±0.01 (11.4±0.4)
9		inactive (10 μM)
10		0.35±0.06 (13.4±0.5)
11		0.41±0.1 (20.6±0.7)
12		inactive (30 μM)
13		0.22±0.03 (16.2±0.3)
14		0.0072±0.0002 (14.1±0.1)
15		0.46±0.03 (11.8±0.2)

Next, we investigated the impact on FXR activation of alternative 4-substituents compared to methoxy derivative **6** which showed antagonistic potency. Replacement of the methoxy group of **6** with a phenolic hydroxyl group in **9** caused inactivity on FXR. A bromine atom in position 4 (**10**) again produced a potent partial FXR agonist with improved EC₅₀ value compared to the unsubstituted derivative **5** which indicated that larger substituents at this position were required. Similar partial agonistic activity was observed for the 4-chlorine derivative **11**. The FXR transactivation activity of **11** furthermore suggested that substituents in position 4 of the 3-aromatic ring were tolerated. Interestingly, a change in the geometry of the central ring compared to **6** and introduction of a hydrophilic substituent as in the 4-hydroxythiazole **12** caused inactivity on FXR again. In contrast to the isoxazole moiety of GW4064 (**3**) and the here reported oxadiazoles, the central thiazole residue of **12** generates a quite linear molecule and does not provide an angle that seems favorable for FXR activation.¹⁸

Finally, we introduced a carboxylic acid moiety at the 4-position of the 5-phenyl substituent combined with the beneficial 2-methylphenyl residue as second aromatic ring. The resulting derivative **13** displayed the best FXR partial agonistic profile amongst **4-13**. Moving the carboxylic acid from position 4 to 3 in **14** strongly enhanced the activity and led to a highly potent partial FXR agonist with an EC₅₀ value of 7.2±0.2 nM. With its low nanomolar partial FXR agonistic activity **14** displayed a promising FXR ligand for further *in vitro* characterization.

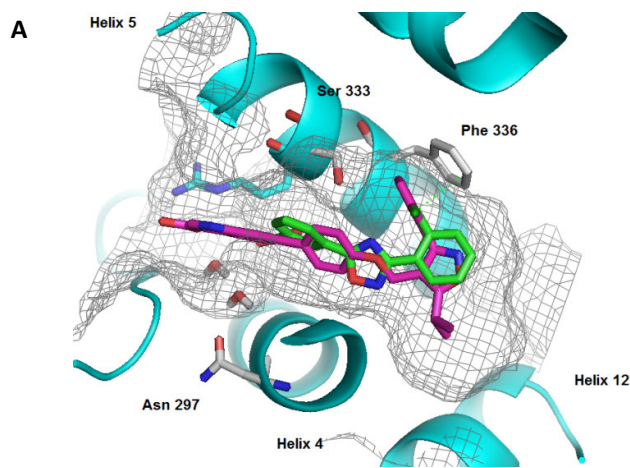
In addition to the highly potent partial FXR agonist **14**, we also obtained a fluorescent FXR ligand **15** by introduction of a coumarin-derived fluorophore as 5-substituent of the central oxadiazole moiety. Compound **15** exhibited nanomolar partial FXR agonism and can serve as fluorescent pharmacological tool for various *in vitro* experiments and assays related to FXR. **15** revealed good fluorescence properties with an absorption maximum at 400 nm and strong fluorescence emission at 480 nm in aqueous solution. In contrast to many known fluorescent ligands of other targets, **15** has the advantage that the fluorophore is part of the compound's pharmacophore instead of being attached with a linker. The solubility of **15** in 1% aq DMSO of >10 mg/L (>28 μM) exceeds the compounds potency (EC₅₀ = 0.46 μM) by more than a factor 60 which is ideal for *in vitro* assays on purified protein. The solution is also stable for at least 4 hours. Hence, **15** might be useful for test systems such as fluorescence polarization.

Summing up, our structure-activity relationship studies suggest that the central oxadiazole moiety of the here reported compounds constitutes a valuable scaffold for novel FXR ligands. Similar to the isoxazole residue of GW4064 (**3**), the oxadiazole ring seems to place its substituents in a favorable angle for binding to the FXR ligand binding site. Our results furthermore indicate that as 5-substituent of this central moiety various residues are tolerated since even the large and sterically demanding fluorophore of **15** did not entirely disrupt the transactivation activity on FXR. Concerning the substituent in position 3 of the oxadiazole, a 2-tolyl moiety which probably causes steric interactions with the neighboring oxadiazole and imitates the 2,6-dichlorophenyl residue of GW4064 (**3**) showed the best FXR transactivation characteristics. This preliminary SAR study presents the class of oxadiazoles as valuable FXR ligands and has yielded **14** and **15** as two promising compounds for further studies and structural optimization.

2.3. Receptor-ligand docking & *in vitro* characterization

We characterized partial FXR agonist **14** *in vitro* to evaluate its pharmacological profile and suitability for further *in vitro* and

in vivo studies. We also investigated the putative binding mode of **14** by automated docking of **14** (Figure 2A) to a model of the FXR-LBD derived from the co-crystal structure of **3a** (PDB-ID: 3RUU²¹). The docking pose suggested a slightly different binding mode than observed for the minimal fragment **4** which might be due to the presence of a carboxylic acid group in **14** that is not tolerated in the lipophilic space near helices 11 and 12. In the docking model, **14** forms polar interactions with Ser333 and a water cluster associated with Asn297 as well as several hydrophobic contacts involving e.g. Phe336. The lipophilic 3-substituent of the oxadiazole moiety was directed towards helix 12 (AF-2).



B

EC₅₀(hFXR) = 7.2±0.2 nM; pEC₅₀ = 8.14
 MW = 280.3 clogP = 3.72; aq. sol. = 33 mg/L (0.12 mM)
 tPSA: 71.3 Å²; HBD: 1; HBA: 5; LE: 0.54; SILE: 3.27
 non-toxic ≤ 50 μM (HepG2; LDH, WST-1)
 metabolic stability: 54±1% after 60 min.

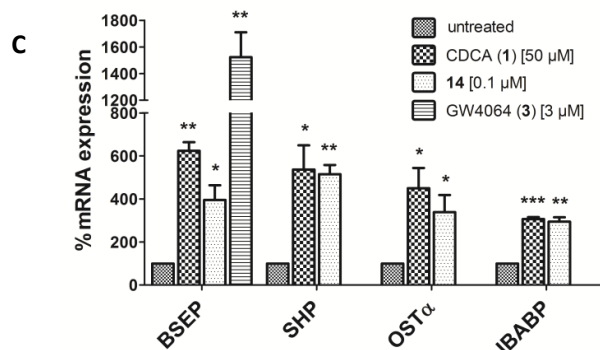


Figure 2: *In vitro* characteristics of **14**: (A) Docking pose of **14** (green, model from PDB-ID: 3RUU²¹, superimposed with **3a** (pink)). (B) Properties of **14** (HBD: H-bond-donors; HBA: H-bond-acceptors). (C) FXR target gene quantification (qRT-PCR): results (mean±SEM; n=4; untreated = 100%): BSEP (bile salt export protein): CDCA [50 μM]: 624±41%; GW4064 [3 μM]: 1523±187%; **14** [0.1 μM]: 395±69%. SHP (small hetero-dimer partner): CDCA [50 μM]: 537±113%; **14** [0.1 μM]: 515±43%. OSTα (organic solute transporter α): CDCA [50 μM]: 450±94%; **14** [0.1 μM]: 339±80%. IBABP (ileal bile acid binding protein): CDCA [50 μM]: 306±10%; **14** [0.1 μM]: 295±20%. * p < 0.05; ** p < 0.01; *** p < 0.001

14 displayed a high aqueous solubility of 33 mg/L (0.12 mM) and acceptable metabolic stability in Sprague-Dawley rat liver microsomes with 54±1% of the compound remaining after 60 minutes incubation (results of the metabolism experiments

(mean±SEM; n=4): 0 min: 99.4 ± 1.4%, 15 min: 84.6 ± 1.5%, 30 min: 71.3 ± 1.1%, 60 min: 53.9 ± 0.9%).

In HepG2 cells the compound revealed low toxic effects with a slight acute toxicity in an lactate dehydrogenase release (LDH) assay at 50 μM and no anti-proliferative effects in the water soluble tetrazolium 1 (WST-1) assay up to 50 μM (results as mean±SEM; n=4: LDH: untreated = 0%, Triton X-100 (2%) = 100%; **14**: 5 μM: 0±3%, 10 μM: 0±3%, 50 μM: 15±4%; WST-1: untreated = 100%; **14**: 5 μM: 109±21%, 10 μM: 87±19%, 50 μM: 86±21%; Figure 2B).

To obtain more evidence on the mode of FXR activation of **14** in a less artificial setting than the reporter gene assay, we performed target gene analysis (Figure 2C) in HepG2 and HT-29 cells after stimulation of the cells with **14** (0.1 μM). Target gene quantification was performed by quantitative real-time PCR using the comparative ΔΔCt method.²⁹ **14** induced the expression of the FXR target genes bile salt export protein (BSEP), small heterodimer partner (SHP) and organic solute transporter α (OSTα) in HepG2 cells and the expression of ileal bile acid binding protein (IBABP) in HT-29 cells. This FXR agonistic activity was comparable in its amplitude with the effect of the physiological FXR agonist CDCA (**1**, 50 μM) thereby corroborating **14** as functional FXR agonist. Concerning BSEP expression, **14** exhibited a slightly lower activation than CDCA (**1**) and a considerably lower activation than GW4064 (**3**, 3 μM). Our results are in agreement with earlier reports that have shown GW4064 (**3**) significantly more effective in inducing BSEP expression than CDCA (**1**) in HepG2 cells as well as in BSEP promoter based reporter gene assays.^{30,31} This fact explains the low maximum relative activation of **14** in the reporter gene assay compared to that of **3** because the reporter luciferase was under the control of a BSEP promoter as well.

3. Conclusion & Outlook

We discovered compound **14** as a highly potent FXR agonist and compound **15** as a related fluorescent FXR ligand by fragmentation of FXR agonist GW4064 (**3**) and subsequent structure-based optimization. Concerning its lower EC₅₀ value and lower molecular weight **14** is superior to its predecessor GW4064 (**3**). Moreover, compound **14** displays low toxicity, high aqueous solubility and good metabolic stability, which make it a valuable compound for further *in vitro* and *in vivo* studies on FXR ligands and the pharmacological role of the nuclear receptor. The fluorescent FXR ligand **15** might become a pharmacological tool for various *in vitro* experiments. **15** combines useful characteristics as a labeled FXR ligand due to its absorption/emission characteristics, low EC₅₀ value, low molecular weight and straightforward synthetic accessibility. With these unique properties both GW4064-derived FXR ligands **14** and **15** resulting from this work constitute new FXR-targeting agents. They have potential to serve as lead compounds and pharmacological tools and help promote FXR-related research.

4. Experimental

4.1. *In vitro* biological evaluation

4.1.1. Full length FXR transactivation assay

HeLa cells were grown in DMEM high glucose supplemented with 10% FCS, SP (1 mM), penicillin (100 U/mL) and streptomycin (100 μg/mL) at 37°C and 5% CO₂.

pcDNA3-hFXR contains the sequence of human FXR and was already published elsewhere³², pGL3basic (Promega Corporation, Fitchburg, WI, USA) was used as a reporter plasmid, with a shortened construct of the promoter of the bile salt export protein

(BSEP, sequence of construct from³³) cloned into the SacI/NheI cleavage site in front of the luciferase gene. pRL-SV40 (Promega Corporation) was transfected as a control for normalization of transfection efficiency and cell growth. pSG5-hRXR was already published elsewhere³⁴ as well.

24 h before transfection, HeLa cells were seeded in 96-well plates with a density of 8,000 cells per well. 3.5 h before transfection, medium was changed to DMEM high glucose, supplemented with SP (1 mM), penicillin (100 U/mL), streptomycin (100 µg/mL) and 0.5% charcoal-stripped FCS. Transient transfection of HeLa cells with BSEP-pGL3, pRL-SV40 and the expression plasmids pcDNA3-hFXR and pSG5-hRXR was carried out using calcium phosphate transfection method. 16 h after transfection, medium was changed to DMEM high glucose, supplemented with SP (1 mM), penicillin (100 U/mL), streptomycin (100 µg/mL) and 0.5% charcoal-stripped FCS. 24 h after transfection, medium was changed to DMEM without phenol red, supplemented with SP (1 mM), penicillin (100 U/mL), streptomycin (100 µg/mL), L-glutamine (2 mM) and 0.5% charcoal-stripped FCS, now additionally containing 0.1% DMSO and the respective test compound or 0.1% DMSO alone as untreated control. Each concentration was tested in triplicate wells and each experiment was repeated independently at least three times. Following 24 h incubation with the test compounds, cells were assayed for luciferase activity using Dual-GloTM Luciferase Assay System (Promega Corporation) according to the manufacturer's protocol. Luminescence was measured with a Tecan Infinite M200 luminometer (Tecan Deutschland GmbH, Crailsheim, Germany). Normalization of transfection efficiency and cell growth was done by division of firefly luciferase data by renilla luciferase data resulting in relative light units (RLU). Fold activation was obtained by dividing the mean RLU of the tested compound at a respective concentration by the mean RLU of untreated control. Relative activation was obtained by dividing the fold activation of the tested compound at a respective concentration by the fold activation of FXR full agonist GW4064 (**3**) at 3 µM. EC₅₀ and standard error of the mean values were calculated with the mean relative activation values of at least three independent experiments by SigmaPlot 10.0 (Systat Software GmbH, Erkrath, Germany) using a four parameter logistic regression.

4.1.2. FXR target gene quantification

HepG2 cells were seeded in DMEM high glucose, supplemented with 10% FCS, SP (1 mM), penicillin (100 U/mL) and streptomycin (100 µg/mL) at 37°C and 5% CO₂ in 6-well plates (2 * 10⁶ per well). HT-29 cells were seeded in McCoy's 5A medium, supplemented with 10% FCS, penicillin (100 U/mL) and streptomycin (100 µg/mL) at 37°C and 5% CO₂ in 6-well plates (2 * 10⁶ per well). 24 h after seeding, medium was changed to MEM, supplemented with 1% charcoal-stripped FCS, penicillin (100 U/mL), streptomycin (100 µg/mL) and L-glutamine (2 mM). After additional 24 h, medium was changed again to MEM, now additionally containing 0.1% DMSO and the respective test compound **14** (0.1 µM) or CDCA (50 µM) or 0.1% DMSO alone as untreated control. Cells were incubated with the test compounds for 24 h, harvested, washed with cold phosphate buffered saline (PBS) and then directly used for RNA extraction or stored at -80°C.

Two micrograms of total RNA were extracted from HepG2 or HT-29 cells by the Total RNA Mini Kit (R6834-02, Omega Bio-Tek, Inc., Norcross, GA, USA). RNA was reverse-transcribed into cDNA using the High-Capacity cDNA Reverse Transcription Kit (4368814, Thermo Fischer Scientific, Inc., Waltham, MA, USA) according to the manufacturer's protocol.

FXR target gene expression was evaluated by quantitative PCR analysis with a StepOnePlusTM System (Life Technologies) using PowerSYBRGreen (Life Technologies; 12.5 µL per well). The primers have been reported previously²⁹. Each sample was set up in duplicates and repeated in at least four independent experiments. The expression was quantified by the comparative ΔΔCt method.

4.1.3. Cytotoxicity Assays

WST-1 assay (Roche Diagnostics International AG, Rotkreuz, Schweiz) was performed according to manufacturer's protocol. In brief, HepG2 cells were seeded in DMEM high glucose, supplemented with SP (1 mM), penicillin (100 U/mL), streptomycin (100 µg/mL) and 10% FCS in 96-well plates (3 * 10⁴ cells/well). After 24 h, medium was changed to DMEM high glucose, supplemented with penicillin (100 U/mL), streptomycin (100 µg/mL) and 1% charcoal stripped FCS and cells were incubated with **14** (final concentrations 5 µM, 10 µM and 50 µM), Revlotron (100 µM) as positive control, and Zileuton (100 µM) and DMEM/1% DMSO as negative controls. After 48 h, WST reagent (Roche Diagnostics International AG) was added to each well according to manufacturer's instructions. After 45 min incubation, absorption (450 nm/ reference: 620 nm) was determined with a Tecan Infinite M200 luminometer (Tecan Deutschland GmbH). Each experiment was repeated at least four times in triplicates. Results (expressed as mean ± SEM; n=4; untreated = 100%) **14**: 5 µM: 109±21%, 10 µM: 87±19%, 50 µM: 86±21%.

LDH assay (Roche Diagnostics International AG) was performed according to manufacturer's instructions. In brief, HepG2 cells were seeded in DMEM high glucose, supplemented with SP (1 mM), penicillin (100 U/mL), streptomycin (100 µg/mL) and 10% FCS in 96-well plates (3 * 10⁴ cells/well). After 24 h, medium was changed to DMEM high glucose, supplemented with penicillin (100 U/mL), streptomycin (100 µg/mL) and 1% charcoal stripped FCS and cells were incubated with **14** (final concentrations 5 µM, 10 µM and 50 µM) for 48 h. As positive control TRITON X-100 (2%) was added 2 h before measurement. After incubation, supernatant of each well was transferred into a fresh plate and LDH substrate/reagent was added. After 20 min incubation, absorption at measurement (490 nm) and reference (690 nm) wavelength was determined with a Tecan Infinite M200 luminometer (Tecan Deutschland GmbH). All experiments were performed in triplicates and at least in four independent repeats. Results (expressed as mean ± SEM; n=4; untreated = 0%, Triton X-100 (2%) = 100%) **14**: 5 µM: 0±3%, 10 µM: 0±3%, 50 µM: 15±4%.

4.1.4. Metabolism Assay

The solubilized test compound **14** (5 µL, final concentration 10 µM in DMSO) was preincubated at 37 °C in 432 µL of phosphate buffer (0.1 M, pH 7.4) together with a 50 µL NADPH regenerating system (30 mM glucose-6-phosphate, 4 U/mL glucose-6-phosphate dehydrogenase, 10 mM NADP, 30 mM MgCl₂). After 5 min, the reaction was started by the addition of 13 µL of microsome mix from the liver of Sprague–Dawley rats (Invitrogen, Darmstadt, Germany; 20 mg protein/mL in 0.1 M phosphate buffer) in a shaking water bath at 37°C. The reaction was stopped by addition of 250 µL of ice-cold methanol at 0, 15, 30 and 60 min. The samples were diluted with 250 µL of DMSO and centrifuged at 10000 g for 5 min at 4°C. The supernatants were analyzed and test compound was quantified by HPLC: mobile phase: MeOH 83%/H₂O 17%/formic acid 0.1%; flow-rate: 1 mL/min; stationary phase: MultoHigh Phenyl phase, 5 µm, 250 × 4, precolumn, phenyl, 5 µm, 20 × 4; detection wavelength: 330 and 254 nm; injection volume: 50 µL. Control samples were

performed to check the stability of **14** in the reaction mixture: first control was without NADPH, which is needed for the enzymatic activity of the microsomes, second control was with inactivated microsomes (incubated for 20 min at 90°C), third control was without test compound **14** (to determine the baseline). The amounts of the test compound **14** were quantified by an external calibration curve, where data are expressed as means \pm SEM of single determinations obtained in three independent experiments. The metabolism experiment showed the following curve (expressed as mean \pm SEM; n=4): **14**: 0 min: 99.4 \pm 1.4%, 15 min: 84.6 \pm 1.5%, 30 min: 71.3 \pm 1.1%, 60 min: 53.9 \pm 0.9%.

4.1.5. Solubility testing of **15**

15 was dissolved in DMSO (1.0 mg/mL) and 10 μ L of this DMSO solution were added to 990 μ L H₂O. The content of **15** in the resulting 1% DMSO solution was analysed by HPLC and found to be 10.07 \pm 0.01 mg/L (27.8 μ mol/L; n=7). After 4 h, the solution was analysed again and found to have a concentration of 9.98 \pm 0.02 mg/L (n=7). Due to the high crystalline nature of **15**, direct dissolution in H₂O containing 1% DMSO yields lower concentrations.

4.2. Docking procedure

Docking simulations were performed using the Molecular Operating Environment (MOE) (Version 2012.10; The Chemical Computing Group, Montreal, Canada). The crystal structure of FXR (PDB ID: 3RUU²¹) was downloaded from the Protein Data Bank (PDB). Prior to ligand docking one monomer of the dimer crystal structure was isolated and the crystallized ligand was removed. Subsequently, the structure was prepared with Protonate 3D and the active site was isolated using MOE Site Finder. The structures were placed in the site with the Triangle Matcher method, and then ranked with the London dG scoring function. For the energy minimization in the pocket MOE Forcefield Refinement was used and ranked with the GBVI/WSA dG scoring function.

4.3. Chemistry

General. All chemicals were purchased from Sigma-Aldrich, Alfa Aesar or Acros Organics and were used without further purification. Analytical TLC (thin layer chromatography) was performed with TLC plates F254 (Merck, Darmstadt, Germany) with detection using a UV-lamp. A Biotage Initiator 2.0 microwave reactor (Biotage, Uppsala, Sweden) was used. ¹H-NMR spectra were recorded on a Bruker AV 250 (¹H: 250 MHz), a Bruker AV 300 (¹H: 300 MHz) or a Bruker AV 400 (¹H: 400 MHz) spectrometer (Bruker Corporation, Billerica, MA, USA). ¹³C-NMR spectra were recorded on a Bruker AV 250 (¹³C: 63 MHz), a Bruker AV 300 (¹³C: 75 MHz) or a Bruker AV 400 (¹³C: 100 MHz) spectrometer (Bruker Corporation). Chemical shifts (δ) are reported in ppm relative to tetramethylsilane (TMS) as reference; multiplicity: s, singlet; d, doublet; dd, double doublet; t, triplet; m, multiplet; pq, pseudoquartet; approximate coupling constants (*J*) are shown in hertz (Hz). Mass spectra were obtained on a VG Platform II (Thermo Fischer Scientific, Inc.) using electrospray ionization (ESI). High resolution mass spectrometry (HRMS) was performed on a MALDI LTQ Orbitrap XL (Thermo Fisher Scientific, Inc.). Elemental analyses (C, H, N) were measured on a Vario MicroCube (Heraeus Holding GmbH, Hanau, Germany) and were within \pm 0.4% of the theoretical values for all final compounds, which corresponds to \geq 95% purity.

5-Isopropyl-3-phenyl-1,2,4-oxadiazole (4). A solution of isobutyric acid (**17a**) (237 mg, 2.69 mmol, 1.00 eq), HOBt x H₂O (495 mg, 3.23 mmol, 1.20 eq) and EDC x HCl (568 mg, 2.96

mmol, 1.30 eq) in DMF (abs., 5 mL) was stirred at room temperature for 30 min. Then, a solution of (Z)-N'-hydroxybenzamidine (**18a**) (366 mg, 2.69 mmol, 1.00 eq) in DMF (abs., 3 mL) was added and the mixture was heated to 180°C for 20 min by microwave irradiation. The reaction mixture was poured on 10 mL ice and was extracted with dichloromethane (3x35 mL). The combined organic layers were washed with 1N sodium hydroxide and brine and were dried over Na₂SO₄. The solvent was removed in vacuum and the crude product was purified by column chromatography (hexane : ethyl acetate = 50:1 \rightarrow 25:1) to give 129 mg (25%) of a yellow oil.³⁵ ¹H-NMR (250 MHz, CDCl₃): δ = 8.10-8.06 (m, 2H, 2H,6H-ph), 7.50-7.44 (m, 3H, 3H,4H,5H-ph), 3.29 (sep, 1H, ³J = 7.0 Hz, -CH-(CH₃)₂), 1.46 (d, 6H, ³J = 7.0 Hz, -(CH₃)₂); ¹³C-NMR (100 MHz, DMSO-*d*₆): δ = 184.0, 167.3, 131.4, 129.1, 126.9, 126.2, 26.7, 19.7; MALDI-MS: m/z = 189.0 [M+H]⁺; MALDI-HRMS anal. calcd. for C₁₁H₁₂N₂O: m/z = 189.10224, [M+H]⁺, found: m/z = 189.10227 [M+H]⁺; purity \geq 95% as determined by HPLC.

3,5-Diphenyl-1,2,4-oxadiazole (5). A solution of benzoic acid (**17b**) (269 mg, 2.20 mmol, 1.00 eq), HOBt x H₂O (405 mg, 2.64 mmol, 1.20 eq) and EDC x HCl (465 mg, 2.42 mmol, 1.10 eq) in DMF (abs., 5 mL) was stirred at room temperature for 30 min. Then, a solution of (Z)-N'-hydroxybenzamidine (**18a**) (300 mg, 2.20 mmol, 1.00 eq) in DMF (abs., 2 mL) was added and the mixture was heated to 180°C for 20 min by microwave irradiation. The reaction mixture was poured on 10 mL ice and was stirred for 30 min. The precipitate was collected, washed with water and was lyophilized to give 394 mg (80%) of a white solid.³⁵ ¹H-NMR (250 MHz, CDCl₃): δ = 8.25-8.17 (m, 4H, 2 x 2H,6H-ph), 7.64-7.49 (m, 6H, 2 x 3H,4H,5H-ph); ¹³C-NMR (100 MHz, CDCl₃): δ = 175.7, 169.0, 132.7, 131.2, 129.1, 128.8, 128.2, 127.5, 127.0, 124.3; ESI-MS: m/z = 223.04 [M+H]⁺; CHN anal. calcd. for C₁₄H₁₀N₂O: C 75.66, H 4.54, N 12.60, found: C 75.72, H 4.85, N 12.74.

5-(4-Methoxyphenyl)-3-phenyl-1,2,4-oxadiazole (6). A solution of 4-methoxybenzoic acid (**17c**) (1.12 g, 7.35 mmol, 1.00 eq), HOBt x H₂O (1.35 g, 8.81 mmol, 1.20 eq) and EDC x HCl (1.55 g, 8.08 mmol, 1.10 eq) in DMF (abs., 8 mL) was stirred at room temperature for 30 min. Then, a solution of (Z)-N'-hydroxybenzamidine (**18a**) (1.00 g, 7.34 mmol, 1.00 eq) in 5 mL abs. DMF was added and the mixture was heated to 180°C for 20 min by microwave irradiation. The reaction mixture was poured on 50 mL ice and stirred for 30 min. The precipitate was collected, washed with water and lyophilized to give 1.43 g (77%) of a white solid.³⁵ ¹H-NMR (250 MHz, CDCl₃): δ = 8.19-8.15 (m, 4H, 2H,6H-ph, 2H,6H-ph-OMe), 7.52-7.50 (m, 3H, 3H,4H,5H-ph), 7.04 (d, 2H, ³J = 8.8 Hz, 3H,5H-ph-OMe), 3.91 (s, 3H, -OCH₃); ¹³C-NMR (63 MHz, DMSO-*d*₆): δ = 175.2, 168.0, 163.0, 131.5, 129.8, 129.1, 127.0, 126.2, 115.6, 114.9, 55.6; mp = 95.4°C; ESI-MS: m/z = 253.0 [M+H]⁺; MALDI-HRMS anal. calcd. for C₁₅H₁₂N₂O₂: m/z = 253.09715 [M+H]⁺, found: m/z = 253.09753 [M+H]⁺; CHN anal. calcd. for C₁₅H₁₂N₂O₂: C 71.41, H 4.79, N 11.10, found: C 71.23, H 4.76, N 11.03.

5-(4-Methoxyphenyl)-3-(3-(trifluoromethyl)phenyl)-1,2,4-oxadiazole (7). To a solution of 4-methoxybenzoyl chloride (2.20 g, 12.89 mmol, 1.00 eq) in pyridine (abs., 20 mL) (Z)-N'-hydroxy-3-(trifluoromethyl)benzamidine (**18c**) (3.11 g, 15.23 mmol, 1.18 eq) was added and the mixture was heated to reflux for 20 h. After cooling to room temperature, ethanol (25 mL) was added. The resulting white, voluminous precipitate was collected and washed with ethanol to yield 2.64 g of a cotton-like solid (64%).²⁸ ¹H-NMR (250 MHz, DMSO-*d*₆): δ = 8.37 (d, 1H, ³J = 7.8 Hz, 4H-ph-CF₃), 8.31 (s, 1H, 2H-ph-CF₃), 8.16 (d, 2H, ³J =

8.8 Hz, 2*H*,6*H*-ph-OMe), 8.01 (d, 1*H*, $^3J = 7.8$ Hz, 6*H*-ph-CF₃), 7.85 (t, 1*H*, $^3J = 7.8$ Hz, 5*H*-ph-CF₃), 7.20 (d, 2*H*, $^3J = 8.8$ Hz, 3*H*,5*H*-ph-OMe), 3.89 (s, 3*H*, -OCH₃); ¹³C-NMR (63 MHz, DMSO-*d*₆): $\delta = 175.7, 167.2, 163.3, 131.0, 130.7, 130.1, 129.7, 128.2, 127.4, 125.9, 123.4, 115.4, 115.0, 55.7$; mp = 128°C; ESI-MS: *m/z* = 320.9 [M+H]⁺; MALDI-HRMS anal. calcd. for C₁₆H₁₁F₃N₂O₂: *m/z* = 321.08454 [M+H]⁺, found: *m/z* = 321.08486 [M+H]⁺; CHN anal. calcd. for C₁₆H₁₁F₃N₂O₂: C 60.00, H 3.46, N 8.75, found: C 59.96, H 3.50, N 8.65.

5-(4-Methoxyphenyl)-3-*o*-tolyl-1,2,4-oxadiazole (8). To a solution of 4-methoxybenzoyl chloride (2.20 g, 12.89 mmol, 1.00 eq) in pyridine (abs., 20 mL) (*Z*)-*N'*-hydroxy-2-methylbenzamidinium (**18b**) (2.29 g, 15.23 mmol, 1.18 eq) was added and the mixture was heated to reflux for 16 h. After cooling to room temperature, ethanol (25 mL) was added. The resulting white, voluminous precipitate was collected and washed with ethanol to yield 2.85 g of a cotton-like solid (83%). ¹H-NMR (250 MHz, DMSO-*d*₆): $\delta = 8.13$ (d, 2*H*, $^3J = 8.9$ Hz, 2*H*,6*H*-ph-OMe), 7.99 (d, 1*H*, $^3J = 8.8$ Hz, 6*H*-tolyl), 7.52-7.37 (m, 3*H*, 3*H*,4*H*,5*H*-tolyl), 7.20 (d, 2*H*, $^3J = 8.8$ Hz, 3*H*,5*H*-ph-OMe), 3.88 (s, 3*H*, -OCH₃), 2.60 (s, 3*H*, -CH₃); ¹³C-NMR (63 MHz, DMSO-*d*₆): $\delta = 174.2, 168.6, 163.0, 137.4, 131.3, 130.8, 129.8, 129.6, 126.1, 125.6, 115.6, 114.9, 55.6, 21.5$; mp = 89.5°C; ESI-MS: *m/z* = 267.0 [M+H]⁺; MALDI-HRMS anal. calcd. for C₁₆H₁₄N₂O₂: *m/z* = 267.11146 [M+H]⁺, found: *m/z* = 267.11296 [M+H]⁺; CHN anal. calcd. for C₁₆H₁₄N₂O₂*1 H₂O: C 70.97, H 5.40, N 10.34, found: C 70.65, H 5.42, N 10.75.

4-(3-Phenyl-1,2,4-oxadiazol-5-yl)phenol (9). To a cooled solution of 5-(4-methoxyphenyl)-3-phenyl-1,2,4-oxadiazole (**6**) (1.50 g, 5.95 mmol, 1.00 eq) in dichloromethane (abs., 20 mL) boron tribromide (2.30 mL, 23.80 mmol, 4.00 eq) was added at -30°C. The solution was stirred for 16 h without renewing the cooling bath. After quenching with water (25 mL), the organic layer was separated and the aqueous phase was extracted with dichloromethane (3x25 mL). The combined organic layers were washed with NaHCO₃ solution (100 mL) and brine (100 mL), dried over Na₂SO₄ and the solvent was removed in vacuum to give 1.39 g (quant.) of a white solid. ¹H-NMR (250 MHz, DMSO-*d*₆): $\delta = 10.56$ (br s, 1*H*, -OH), 8.09-8.02 (m, 4*H*, 2*H*,6*H*-ph, 3*H*,5*H*-ph-OH), 7.60 (br s, 3*H*, 3*H*,4*H*,5*H*-ph), 7.00 (d, 2*H*, $^3J = 8.3$ Hz, 2*H*,6*H*-ph-OH); ¹³C-NMR (63 MHz, DMSO-*d*₆): $\delta = 175.4, 167.9, 162.0, 131.4, 130.0, 129.1, 126.9, 126.3, 116.2, 114.0$; ESI-MS: *m/z* = 238.7 [M+H]⁺; MALDI-HRMS anal. calcd. for C₁₄H₁₀N₂O₂: *m/z* = 239.08150 [M+H]⁺, found: *m/z* = 239.08191 [M+H]⁺; CHN anal. calcd. for C₁₄H₁₀N₂O₂: C 70.58, H 4.23, N 11.76, found: C 70.50, H 4.25, N 11.53.

5-(4-Bromophenyl)-3-phenyl-1,2,4-oxadiazole (10). To a solution of 4-bromobenzoyl chloride (1.60 g, 7.29 mmol, 1.00 eq) in pyridine (abs., 6 mL) (*Z*)-*N'*-hydroxybenzamidinium (**18a**) (1.17 g, 8.60 mmol, 1.18 eq) was added and the mixture was heated to reflux for 20 h. After cooling to room temperature, ethanol (25 mL) was added. The resulting white, voluminous precipitate was collected and washed with ethanol to yield 1.41 g of a crystalline solid (64%). ¹H-NMR (250 MHz, DMSO-*d*₆): $\delta = 8.12$ -8.06 (m, 4*H*, 2*H*,6*H*-ph, 3*H*,5*H*-ph-Br), 7.87 (d, 2*H*, $^3J = 8.5$ Hz, 2*H*,6*H*-ph-Br), 7.62-7.57 (m, 3*H*, 3*H*,4*H*,5*H*-ph); ¹³C-NMR (63 MHz, DMSO-*d*₆): $\delta = 174.6, 168.2, 132.6, 131.6, 129.7, 129.2, 127.2, 127.0, 125.9, 122.5$; mp = 122.5°C; ESI-MS: *m/z* = 300.8 [M+H]⁺; MALDI-HRMS anal. calcd. for C₁₄H₉BrN₂O₂: *m/z* = 300.99710 [M+H]⁺, found: *m/z* = 300.99764 [M+H]⁺; CHN anal. calcd. for C₁₄H₉BrN₂O₂: C 55.84, H 3.01, N 9.30, found: C 55.83, H 3.09, N 9.12.

5-(4-Chlorophenyl)-3-*p*-tolyl-1,2,4-oxadiazole (11). To a solution of 4-chlorobenzoyl chloride (0.70 g, 4.00 mmol, 1.00 eq)

in pyridine (abs., 50 mL) (*Z*)-*N'*-hydroxy-4-methylbenzamidinium (**18d**) (0.50 g, 3.30 mmol, 1.21 eq) was added and the mixture was heated to reflux for 16 h. The solvent was removed in vacuum and the residue was recrystallized from water:methanol to yield 0.41 g of a white solid (46%). ¹H-NMR (250 MHz, DMSO-*d*₆): $\delta = 8.29$ (d, 2*H*, $^3J = 8.1$ Hz, 2*H*,6*H*-tolyl), 8.08 (d, 2*H*, 2*H*,6*H*-ph-Cl), 7.86 (d, 2*H*, 3*H*,5*H*-ph-Cl), 7.52 (d, 2*H*, 3*H*,5*H*-tolyl), 2.51 (s, 3*H*, -CH₃); ¹³C-NMR (63 MHz, DMSO-*d*₆): $\delta = 174.3, 168.2, 155.1, 141.6, 138.0, 129.7, 129.6, 126.9, 123.1, 122.2, 21.0$; mp = 149°C; ESI-MS: *m/z* = 271.1 [M+H]⁺; CHN anal. calcd. for C₁₅H₁₁ClN₂O: C 66.55, H 4.10, N 10.35, found: C 66.59, H 4.09, N 10.38.

5-(4-Methoxyphenyl)-2-*p*-tolyl-1,3-thiazol-4-ol (12). A mixture of 4-methylbenzimidazole (**23**) (0.33 g, 2.77 mmol, 1.00 eq), 2-mercapto-2-(4-methoxyphenyl)acetic acid (**22**) (0.55 g, 2.77 mmol, 1.00 eq) and triethylamine (1.00 mL, 7.21 mmol, 2.60 eq) was heated to 100°C for 25 min by microwave irradiation. The solvent was removed under reduced pressure and the residue was recrystallized from methanol to yield 102 mg (12%) of a yellow solid. ¹H-NMR (250 MHz, DMSO-*d*₆): $\delta = 11.30$ (br s, 1*H*, -OH), 7.75 (d, 2*H*, $^3J = 8.1$ Hz, 2*H*,6*H*-tolyl), 7.63 (d, 2*H*, $^3J = 8.9$ Hz, 2*H*,6*H*-ph-OMe), 7.30 (d, 2*H*, 3*H*,5*H*-tolyl), 6.97 (d, 2*H*, $^3J = 8.9$ Hz, 3*H*,5*H*-ph-OMe), 3.77 (s, 3*H*, -OCH₃), 2.35 (s, 3*H*, -CH₃); ¹³C-NMR (63 MHz, DMSO-*d*₆): $\delta = 158.6, 157.6, 157.2, 139.8, 130.5, 129.8, 127.3, 125.0, 124.3, 114.3, 107.1, 55.1, 20.9$; mp = 226.7°C; ESI-MS: *m/z* = 298.2 [M+H]⁺; Anal. calcd. for C₁₇H₁₅NO₂S: C 68.66, H 5.08, N 4.71, S 10.78, found: C 68.74, H 5.03, N 4.67, S 10.97.

4-(3-*o*-Tolyl-1,2,4-oxadiazol-5-yl)benzoic acid (13). A solution of terephthalic acid (**17f**) (0.33 g, 2.00 mmol, 1.50 eq), HOBt x H₂O (0.31 g, 2.00 mmol, 1.50 eq) and EDC x HCl (0.38 g, 2.00 mmol, 1.50 eq) in DMF (abs., 5 mL) was stirred at room temperature for 30 min. Then, a solution of (*Z*)-*N'*-hydroxy-2-methylbenzamidinium (**18b**) (200 mg, 1.33 mmol, 1.00 eq) in DMF (abs., 3 mL) was added and the mixture was heated to 180°C for 20 min by microwave irradiation. The reaction mixture was poured on ice (10 g) and was stirred for 30 min. The precipitate was collected, washed with water and lyophilized. The crude product was recrystallized from methanol to give 214 mg (57%) of a white solid. ¹H-NMR (250 MHz, DMSO-*d*₆): $\delta = 13.49$ (br s, 1*H*, -COOH), 8.31 (d, 2*H*, $^3J = 8.3$ Hz, 2*H*,6*H*-ph-COOH), 8.19 (d, 2*H*, $^3J = 8.3$ Hz, 3*H*,5*H*-ph-COOH), 8.02 (d, 1*H*, $^3J = 7.0$ Hz, 6*H*-tolyl), 7.54-7.39 (m, 3*H*, 3*H*,4*H*,5*H*-tolyl), 2.62 (s, 3*H*, -CH₃); ¹³C-NMR (100 MHz, DMSO-*d*₆): $\delta = 173.6, 169.0, 166.3, 137.5, 134.6, 131.4, 131.0, 130.2, 129.7, 128.1, 126.7, 126.2, 125.3, 21.5$; ESI-MS: *m/z* = 279.1 [M-H]⁻; CHN anal. calcd. for C₁₆H₁₂N₂O₃: C 68.56, H 4.32, N 9.99, found: C 68.93, H 4.52, N 10.27.

3-(3-*o*-Tolyl-1,2,4-oxadiazol-5-yl)benzoic acid (14). A solution of isophthalic acid (**17g**) (332 mg, 2.00 mmol, 1.50 eq), HOBt x H₂O (306 mg, 2.00 mmol, 1.50 eq) and EDC x HCl (383 mg, 2.00 mmol, 1.50 eq) in DMF (abs., 5 mL) was stirred at room temperature for 30 min. Then, a solution of (*Z*)-*N'*-hydroxy-2-methylbenzamidinium (**18b**) (200 mg, 1.33 mmol, 1.00 eq) in DMF (abs., 3 mL) was added and the mixture was heated to 180°C for 20 min under microwave irradiation. The reaction mixture was poured on 10 mL ice and stirred for 30 min. The precipitate was collected, washed with water and lyophilized. The crude product was dissolved in methanol, solids were removed and the solution was titrated with water. The precipitate was collected, washed with water and dried to give 84 mg (23%) of a colorless solid. ¹H-NMR (250 MHz, DMSO-*d*₆): 13.52 (s, 1*H*, -OH), 8.69 (s, 1*H*, 2*H*-ph), 8.43 (d, 1*H*, $^3J = 8.0$ Hz, 4*H*-ph), 8.27 (d, 1*H*, $^3J = 8.0$ Hz, 6*H*-ph); 8.05 (d, 1*H*, $^3J = 7.5$

Hz, 6*H*-ph⁺), 7.82 (t, 1H, ³*J* = 7.5 Hz, 5*H*-ph), 7.52 (t, 1H, ³*J* = 7.5 Hz, 5*H*-ph⁺), 7.47-7.41(m, 2H, 3*H*,4*H*-ph⁺), 2.63 (s, 3H, -CH₃); ¹³C-NMR (100 MHz, DMSO-*d*₆): δ = 173.6, 166.1, 137.5, 133.6, 132.1, 131.8, 131.4, 131.0, 130.1, 129.8, 128.4, 126.2, 125.3, 123.8, 58.5, 21.5; ESI-MS: *m/z* = 320.7 [M+K]⁺, 263.6 [M-H₂O+H]⁺; CHN anal. calcd. for C₁₆H₁₂N₂O₃: C 68.56, H 4.32, N 9.99, found: C 68.57, H 4.50, N 10.11.

7-(Diethylamino)-3-(3-phenyl-1,2,4-oxadiazol-5-yl)-2*H*-chromen-2-one (15). A solution of 7-(diethylamino)-2-oxo-2*H*-chromene-3-carboxylic acid (**21**) (250 mg, 0.96 mmol, 1.00 eq), HOBT x H₂O (147 mg, 0.96 mmol, 1.00 eq) and EDC x HCl (0.17 mL, 0.96 mmol, 1.00 eq) in DMF (abs., 5 mL) was stirred at room temperature for 30 min. Then, a solution of (*Z*)-*N'*-hydroxybenzamidine (**18a**) (130 mg, 1.33 mmol, 1.00 eq) in DMF (abs., 3 mL) was added and the mixture was heated to 150°C for 20 min under microwave irradiation. The reaction mixture was poured on 35 mL ice and stirred for 45 min. The precipitate was collected, washed with water and lyophilized to give 283 mg (57%) of a yellow solid.³⁷ ¹H-NMR (250 MHz, CDCl₃): δ = 8.64 (s, 1H, CH=C), 8.20-8.16 (m, 2H, 2*H*,6*H*-ph), 7.51-7.42 (m, 4H, 3*H*,4*H*,5*H*-ph + 5*H*-chromene), 6.66 (dd, 1H, ³*J* = 8.6 Hz, ⁴*J* = 2.4 Hz, 6*H*-chromene), 6.53 (d, 1H, ⁴*J* = 2.2 Hz, 8*H*-chromene), 3.46 (q, 4H, ³*J* = 7.1 Hz, N-(CH₂-CH₃)₂), 1.26 (t, 6H, ³*J* = 7.1 Hz, N-(CH₂-CH₃)₂); ¹³C-NMR (63 MHz, CDCl₃): δ = 173.5, 167.5, 158.0, 156.7, 153.2, 147.7, 132.0, 131.5, 129.2, 127.0, 126.4, 110.3, 107.5, 102.0, 96.1, 44.5, 12.4; ESI-MS: *m/z* = 362.4 [M+H]⁺; CHN anal. calcd. for C₂₁H₁₉N₃O₃*0.5 H₂O: C 68.09, H 5.44, N 11.34, found: C 67.89, H 5.34, N 11.38.

(*Z*)-*N'*-Hydroxybenzamidine (18a). A suspension of benzonitrile (**16a**) (10.00 g, 96.97 mmol, 1.00 eq), hydroxylamine hydrochloride (8.76 g, 126.05 mmol, 1.30 eq) and sodium carbonate (13.36 g, 126.05 mmol, 1.30 eq) in ethanol (abs., 100 mL) was heated to reflux for 17 h. After 3 h further hydroxylamine hydrochloride (1.30 eq) and sodium carbonate (1.30 eq) were added. The inorganic solids were removed by filtration and the solvent was removed in vacuum to give 13.20 g of a colorless oil that solidifies over time (quant.).²⁶ ¹H-NMR (250 MHz, DMSO-*d*₆): δ = 9.61 (s, 1H, -OH), 7.68-7.65 (m, 2H, 2*H*,6*H*-ph), 7.38-7.35 (m, 3H, 3*H*,4*H*,5*H*-ph), 5.79 (s, 2H, NH₂); ESI-MS: *m/z* = 136.6 [M+H]⁺.

(*Z*)-*N'*-Hydroxy-2-methylbenzamidine (18b). A suspension of 2-methylbenzonitrile (**16b**) (5.00 mL, 42.68 mmol, 1.00 eq), hydroxylamine hydrochloride (3.78 g, 54.38 mmol, 1.30 eq) and sodium carbonate (5.76 g, 54.38 mmol, 1.30 eq) in ethanol (abs., 40 mL) was heated to reflux for 16 h. After 3 h, further hydroxylamine hydrochloride (1.30 eq) and sodium carbonate (1.30 eq) were added. The inorganic solids were removed by filtration and the solvent was removed in vacuum to give 3.95 g of a colorless oil that solidifies over time (63%).²⁶ ¹H-NMR (250 MHz, DMSO-*d*₆): δ = 9.31 (s, 1H, -OH), 7.30-7.18 (m, 4H, 3*H*,4*H*,5*H*,6*H*-tolyl), 5.71 (s, 2H, NH₂), 2.34 (s, 3H, CH₃); ESI-MS: *m/z* = 150.6 [M+H]⁺.

(*Z*)-*N'*-Hydroxy-3-(trifluoromethyl)benzamidine (18c). A suspension of 3-(trifluoromethyl)benzonitrile (**16c**) (2.35 mL, 17.53 mmol, 1.00 eq), hydroxylamine hydrochloride (1.58 g, 22.79 mmol, 1.30 eq) and sodium carbonate (2.42 g, 22.79 mmol, 1.30 eq) in ethanol (abs., 20 mL) was heated to reflux for 22 h. After 3 h, further hydroxylamine hydrochloride (1.30 eq) and sodium carbonate (1.30 eq) were added. The inorganic solids were removed by filtration and the solvent was removed in vacuum to give 3.60 g of a colorless oil that solidifies over time (quant.).²⁶ ¹H-NMR (250 MHz, CDCl₃): δ = 7.90 (s, 1H, 2*H*-ph-CF₃), 7.82 (d, 1H, ³*J* = 7.8 Hz, 4*H*-ph-CF₃), 7.68 (d, 1H, ³*J* = 7.8

Hz, 6*H*-ph-CF₃), 7.53 (t, 1H, ³*J* = 7.8 Hz, 5*H*-ph-CF₃), 4.92 (br s, 2H, NH₂), 1.89 (s, 1H, -OH); ESI-MS: *m/z* = 204.6 [M+H]⁺.

(*Z*)-*N'*-Hydroxy-4-methylbenzamidine (18d). A suspension of 4-methylbenzonitrile (**16d**) (1.71 g, 10.00 mmol, 1.00 eq), hydroxylamine hydrochloride (0.90 g, 13.00 mmol, 1.30 eq) and sodium carbonate (1.38 g, 13.00 mmol, 1.30 eq) in ethanol (abs., 30 mL) was heated to reflux for 17 h. After 3 h further hydroxylamine hydrochloride (1.30 eq) and sodium carbonate (1.30 eq) were added. The inorganic solids were removed by filtration and the solvent was removed in vacuum to give 0.94 g of a white solid (63%).²⁶ ¹H-NMR (250 MHz, DMSO-*d*₆): δ = 9.57 (s, 1H, -OH), 7.58 (d, 2H, ³*J* = 8.1 Hz, 3*H*,5*H*-tolyl), 7.19 (d, 2H, ³*J* = 8.0 Hz, 2*H*,6*H*-tolyl), 5.72 (s, 2H, NH₂), 2.32 (s, 3H, -CH₃); ESI-MS: *m/z* = 151.2 [M+H]⁺.

7-(Diethylamino)-2-oxo-2*H*-chromene-3-carboxylic acid (21). A suspension of 4-(diethylamino)-2-hydroxybenzaldehyde (**19**) (1.00 g, 5.18 mmol, 1.00 eq), meldrum's acid (**20**) (0.75 g, 5.18 mmol, 1.00 eq), piperidine (0.04 g, 0.52 mmol, 0.10 eq) and two drops of acetic acid in ethanol (abs., 8 mL) was stirred for 30 min at room temperature and heated to reflux for 3 h. The reaction mixture was concentrated in vacuum and poured on 15 mL of ice water. The resulting precipitate was collected and washed with ethanol to give 854 mg (63%) of an orange crystalline solid.²⁷ ¹H-NMR (400 MHz, DMSO-*d*₆): δ = 12.50 (br s, 1H, -COOH), 8.58 (s, 1H, CH=C), 7.63 (d, 1H, ³*J* = 9.0 Hz, 5*H*-ph), 6.79 (d, 1H, ³*J* = 9.0 Hz, 6*H*-ph), 6.57 (s, 1H, 8*H*-ph), 3.48 (q, 4H, ³*J* = 7.0 Hz, N-(CH₂-CH₃)₂), 1.14 (t, 6H, ³*J* = 6.9 Hz, N-(CH₂-CH₃)₂); ESI-MS: *m/z* = 260.0 [M-H]⁻.

Acknowledgments

We gratefully acknowledge financial support by the Else-Kröner-Fresenius-Stiftung, Research Training Group Translational Research Innovation Pharma - TRIP and the DFG INST 208/664-1.

References and notes

- Seol, W.; Choi, H.; Moore, D. Isolation of proteins that interact specifically with the retinoid X receptor: two novel orphan receptors. *Mol. Endocrinol.*, **1995**, *9*(1), 72–85.
- Forman, B.; Goode, E.; Chen, J.; Oro, A.; Bradley, D.; Perlmann, T.; Noonan, D.; Burka, L.; McMorris, T.; Lamph, W.; Evans, R.; Weinberger, C. Identification of a nuclear receptor that is activated by farnesol metabolites. *Cell*, **1995**, *81*(5), 687–693.
- Makishima, M.; Okamoto, A.; Repa, J.; Tu, H.; Learned, R.; Luk, A.; Hull, M.; Lustig, K.; Mangelsdorf, D.; Shan, B. Identification of a nuclear receptor for bile acids. *Science*, **1999**, *284*(5418), 1362–1365.
- Parks, D.; Blanchard, S.; Bledsoe, R.; Chandra, G.; Consler, T.; Kliewer, S.; Stimmel, J.; Willson, T.; Zavacki, A.; Moore, D.; Lehmann, J. Bile acids: natural ligands for an orphan nuclear receptor. *Science*, **1999**, *284*(5418), 1365–1368.
- Gadaleta, R. M.; Cariello, M.; Sabbà, C.; Moschetta, A. Tissue-specific actions of FXR in metabolism and cancer. *Biochim. Biophys. Acta*, **2015**, *1851*(1), 30–39.
- Ryan, K.; Tremaroli, V.; Clemmensen, C.; Kovatcheva-Datchary, P.; Myronovych, A.; Kams, R.; Wilson-Pérez, H.; Sandoval, D.; Kohli, R.; Bäckhed, F.; Seeley, R. FXR is a molecular target for the effects of vertical sleeve gastrectomy. *Nature*, **2014**, *509*(7499), 183–188.
- Hollman, D.; Milona, A.; van Erpecum, K.; van Mil, S. Anti-inflammatory and metabolic actions of FXR: insights into molecular mechanisms. *Biochim. Biophys. Acta*, **2012**, *1821*(11), 1443–1452.
- Nijmeijer, R.; Gadaleta, R.; van Mil, S.; van Bodegraven, A.; Crusius, J.; Dijkstra, G.; Hommes, D.; de Jong, D.; Stokkers, P.; Verspaget, H.; Weersma, R.; van der Woude, C.; Stapelbroek, J.; Schipper, M.; Wijmenga, C.; van Erpecum, K.; Oldenburg, B.

- Farnesoid X receptor (FXR) activation and FXR genetic variation in inflammatory bowel disease. *PLoS ONE*, **2011**, 6(8), e23745.
9. Goodwin, B.; Jones, S.; Price, R.; Watson, M.; McKee, D.; Moore, L.; Galardi, C.; Wilson, J.; Lewis, M.; Roth, M.; Maloney, P.; Willson, T.; Kliewer, S. A regulatory cascade of the nuclear receptors FXR, SHP-1, and LRF-1 represses bile acid biosynthesis. *Mol. Cell*, **2000**, 6(3), 517–526.
 10. Gioiello, A.; Cerra, B.; Mostarda, S.; Guercini, C.; Pellicciari, R.; Macchiariulo, A. Bile Acid Derivatives as Ligands of the Farnesoid X Receptor: Molecular Determinants for Bile Acid Binding and Receptor Modulation. *Curr. Top. Med. Chem.* **2014**, 14(19), 2159–2174.
 11. Zhang, Y.; Edwards, P. A. FXR signaling in metabolic disease. *FEBS Lett.*, **2008**, 582(1), 10–18.
 12. Adorini, L.; Pruzanski, M.; Shapiro, D. Farnesoid X receptor targeting to treat nonalcoholic steatohepatitis. *Drug Discov. Today*, **2012**, 17(17–18), 988–997.
 13. Fan, M.; Wang, X.; Xu, G.; Yan, Q.; Huang, W. Bile acid signaling and liver regeneration. *Biochim. Biophys. Acta*, **2014**, doi: 10.1016/j.bbagr.2014.05.021.
 14. Trauner, M.; Halilbasic, E. Nuclear receptors as new perspective for the management of liver diseases. *Gastroenterology*, **2011**, 140(4), 1120–1125.
 15. Carotti, A.; Marinuzzi, M.; Custodi, C.; Cerra, B.; Pellicciari, R.; Gioiello, A.; Macchiariulo, A. Beyond Bile Acids: Targeting Farnesoid X Receptor (FXR) with Natural and Synthetic Ligands. *Curr. Top. Med. Chem.* **2014**, 14(19), 2129–2142.
 16. Pellicciari, R.; Fiorucci, S.; Camaioni, E.; Clerici, C.; Costantino, G.; Maloney, P.; Morelli, A.; Parks, D.; Willson, T. 6 α -ethyl-chenodeoxycholic acid (6-ECDC), a potent and selective FXR agonist endowed with anticholestatic activity. *J. Med. Chem.*, **2002**, 45(17), 3569–3572.
 17. Mudaliar, S.; Henry, R.; Sanyal, A.; Morrow, L.; Marschall, H.; Kipnes, M.; Adorini, L.; Sciacca, C.; Clopton, P.; Castelloe, E.; Dillon, P.; Pruzanski, M.; Shapiro, D. Efficacy and safety of the farnesoid X receptor agonist obeticholic acid in patients with type 2 diabetes and nonalcoholic fatty liver disease. *Gastroenterology*, **2013**, 145(3), 574–82.
 18. Merk, D.; Steinhilber, D.; Schubert-Zsilavecz, M. Medicinal chemistry of farnesoid X receptor ligands: from agonists and antagonists to modulators. *Future Med. Chem.*, **2012**, 4(8), 1015–1036.
 19. Howarth, D.; Law, S.; Law, J.; Mondon, J.; Kullman, S.; Hinton, D. Exposure to the synthetic FXR agonist GW4064 causes alterations in gene expression and sublethal hepatotoxicity in eleutheroembryo medaka (*Oryzias latipes*). *Toxicol. Appl. Pharmacol.*, **2010**, 243(1), 111–121.
 20. Maloney, P.; Parks, D.; Haffner, C.; Fivush, A.; Chandra, G.; Plunket, K.; Creech, K.; Moore, L.; Wilson, J.; Lewis, M.; Jones, S.; Willson, T. Identification of a chemical tool for the orphan nuclear receptor FXR. *J. Med. Chem.*, **2000**, 43(16), 2971–2974.
 21. Akwabi-Ameyaw, A.; Bass, J.; Caldwell, R.; Caravella, J.; Chen, L.; Creech, K.; Deaton, D.; Jones, S.; Kaldor, I.; Liu, Y.; Madauss, K.; Marr, H.; McFadyen, R.; Miller, A.; Iii, F.; Parks, D.; Spearing, P.; Todd, D.; Williams, S.; Wisely, G. Conformationally constrained farnesoid X receptor (FXR) agonists: Naphthoic acid-based analogs of GW 4064. *Bioorg. Med. Chem. Lett.*, **2008**, 18(15), 4339–4343.
 22. Gege, C.; Kinzel, O.; Steeneck, C.; Schulz, A.; Kremoser, C. Knocking on FXR's Door: The "Hammerhead"-Structure Series of FXR Agonists - Amphiphilic Isoxazoles with Potent In Vitro and In Vivo Activities. *Curr. Top. Med. Chem.* **2014**, 14(19), 2143–2158.
 23. Akwabi-Ameyaw, A.; Bass, J.; Caldwell, R.; Caravella, J.; Chen, L.; Creech, K.; Deaton, D.; Madauss, K.; Marr, H.; McFadyen, R.; Miller, A.; Navas, F.; Parks, D.; Spearing, P.; Todd, D.; Williams, S.; Bruce Wisely, G. FXR agonist activity of conformationally constrained analogs of GW 4064. *Bioorg. Med. Chem. Lett.*, **2009**, 19(16), 4733–4739.
 24. Akwabi-Ameyaw, A.; Caravella, J.; Chen, L.; Creech, K.; Deaton, D.; Madauss, K.; Marr, H.; Miller, A.; Navas, F.; Parks, D.; Spearing, P.; Todd, D.; Williams, S.; Wisely, G. Conformationally constrained farnesoid X receptor (FXR) agonists: Alternative replacements of the stilbene. *Bioorg. Med. Chem. Lett.*, **2011**, 21(20), 6154–6160.
 25. Feng, S.; Yang, M.; Zhang, Z.; Wang, Z.; Hong, D.; Richter, H.; Benson, G.; Bleicher, K.; Grether, U.; Martin, R.; Plancher, J.; Kuhn, B.; Rudolph, M.; Chen, L. Identification of an N-oxide pyridine GW4064 analog as a potent FXR agonist. *Bioorg. Med. Chem. Lett.*, **2009**, 19(9), 2595–2598.
 26. Katritzky, A.; Shestopalov, A.; Suzuki, K. A convenient synthesis of chiral 1,2,4-oxadiazoles from N-protected (α -aminoacyl)benzotriazoles. *ARKIVOC*, **2005**, vii, 36–55.
 27. Song, A.; Wang, X.; Lam, K. S. A convenient synthesis of coumarin-3-carboxylic acids via Knoevenagel condensation of Meldrum's acid with ortho-hydroxyaryl aldehydes or ketones. *Tet. Lett.*, **2003**, 44(9), 1755–1758.
 28. Versiani dos Anjos, J.; Sinou, D.; de Melo, S.; Srivastava, R. Synthesis of Ethyl 4-O-[4-(1,2,4-Oxadiazol-5-yl)phenyl]- α -D-mannopyranosides. *Lett. Org. Chem.*, **2007**, 4(6), 393–397.
 29. Merk, D.; Lamers, C.; Ahmad, K.; Carrasco Gomez, R.; Schneider, G.; Steinhilber, D.; Schubert-Zsilavecz, M. Extending the Structure-Activity Relationship of Anthranilic Acid Derivatives As Farnesoid X Receptor Modulators: Development of a Highly Potent Partial Farnesoid X Receptor Agonist. *J. Med. Chem.*, **2014**, 57(19), 8035–8055.
 30. Kassam, A.; Miao, B.; Young, P.; Mukherjee, R. Retinoid X Receptor (RXR) Agonist-induced Antagonism of Farnesoid X Receptor (FXR) Activity due to Absence of Coactivator Recruitment and Decreased DNA Binding. *J. Biol. Chem.* **2003**, 278(12), 10028–10032.
 31. Yu, J.; Lo, J.; Huang, L.; Zhao, A.; Metzger, E.; Adams, A.; Meinke, P.; Wright, S.; Cui, J. Lithocholic Acid Decreases Expression of Bile Salt Export Pump through Farnesoid X Receptor Antagonist Activity. *J. Biol. Chem.* **2002**, 277(35), 31441–31447.
 32. Steri, R.; Achenbach, J.; Steinhilber, D.; Schubert-Zsilavecz, M.; Proschak, E. Investigation of imatinib and other approved drugs as starting points for antidiabetic drug discovery with FXR modulating activity. *Biochem. Pharmacol.* **2012**, 83 (12), 1674–1681.
 33. Ananthanarayanan, M.; Balasubramanian, N.; Makishi ma, M.; Mangelsdorf, D. J.; Suchy, F. J. Human bile salt export pump promoter is transactivated by the farnesoid X receptor/bile acid receptor. *J. Biol. Chem.* **2001**, 276 (31), 28857–28865.
 34. Seuter, S.; Väisänen, S.; Rådmark, O.; Carlberg, C.; Steinhilber, D. Functional characterization of vitamin D responding regions in the human 5-Lipoxygenase gene. *Biochim. Biophys. Acta* **2007**, 1771 (7), 864–872.
 35. Montalbetti, C.; Falque, V. Amide bond formation and peptide coupling. *Tetrahedron* **2005**, 61, 10827–10852.
 36. Lill, A.; Rödl, C.; Steinhilber, D.; Stark, H.; Hofmann, B. Development and evaluation of ST-1829 based on 5-benzylidene-2-phenylthiazolones as promising agent for anti-leukotriene therapy. *Eur. J. Med. Chem.* **2015**, 89(1), 503–523.
 37. Detistov, O.; Orlov, V.; Zhuravel' I. Isomeric 3-Isxadiazolylcoumarins and Their Derivatives. *J. Heterocyclic Chem.* **2012**, 49(4), 883–892.